Structural Engineering and Mechanics, *Vol. 61, No. 6 (2017) 775-784*
DOI: https://doi.org/10.12989/sem.2017.61.6.775

Vehicle/track dynamic interaction considering developed railway substructure models

Seyed-Ali Mosayebi[a], Jabbar-Ali Zakeri[b] and Morteza Esmaeili[*]

School of Railway Engineering, Iran University of Science and Technology, Tehran, Iran

(Received November 17, 2015, Revised November 27, 2016, Accepted November 28, 2016)

Abstract. This study is devoted to developing many new substructure models for ballasted railway track by using the pyramid model philosophy. As the effect of railway embankment has been less considered in the previous studies in the field of vehicle/track interaction, so the present study develops the pyramid models in the presence of railway embankment and implements them in vehicle/track interaction dynamic analyses. Considering a moving car body as multi bodies with 10 degrees of freedom and the ballasted track including rail, sleeper, ballast, subgrade and embankment, two categories of numerical analyses are performed by considering the new substructure systems including type A (initiation of stress overlap areas in adjacent sleepers from the ballast layer) or type B (initiation of stress overlap areas in adjacent sleepers from the subgrade layer). A comprehensive sensitivity analyses are performed on effective parameters such as ballast height, sleepers spacing and sleeper width. The results indicate that the stiffness of subgrade, embankment and foundation increased by increasing the ballast height. Also, by increasing the ballast height, rail and ballast vertical displacement decreased.

Keywords: new substructure models; developed pyramid models; railway embankment; vehicle/track interaction; dynamic analysis

1. Introduction

According to increasing the goods and passengers transportation industry in recent years, many countries have paid special attention to rail transport industry as a safe, inexpensive and environment-friendly system compared to other transportation modes. In parallel to developing the transportation technology, extending the precise and modern analysis and design tools seems essential. One of the most advanced analytical methods is modeling the vehicle/track dynamic interaction which has been investigated in the framework of commercial software or the developed codes by various engineers and researchers. For example, Kerr (2000, 2003) investigated the various measuring methods of rail support modulus and its effects on moving train loads. Cai and Raymond (1994) investigated the behavior of railway track as a beam on Winkler foundation caused by wheel and rail forces. Chang and Liu (1996) studied the dynamic behavior of railway track as a beam under a moving load using finite element method. Sun and Dhanasekar (2002) presented a dynamic model for calculation of railway track and wagon system interaction. Ishida and Suzuki (2005) surveyed the settlement of railway track caused by moving axle load. Muscolino and Palmeri (2007) studied the response of railway track as a beam on viscoelastic foundation under the moving oscillators. Uzzal *et al.* (2008) modeled the vehicle-track interaction in ballasted railway track. Zakeri and Xia (2008), Zakeri *et al.* (2009) investigated the track parameters and rail irregularity by considering the railway track model including three layers under the effect of moving train. Rezvani *et al.* (2013) presented an analytical solution for dynamic analysis of railway bridges due to opposing moving trains. Xia *et al.* (2013) analyzed a train-ladder track-bridge dynamic interaction numerically. Berggren (2009) studied the effects of track stiffness on railway behavior. Lei and Zhang (2010) studied the track stiffness by considering rail on the discrete supports. Zakeri and Ghorbani (2011) studied the behavior of transition zone due to moving train loads. In continuation, O'brien *et al.* (2012) investigated the subgrade subsidence by simulation of railway track and train. Esmaeili *et al.* (2014) studied the ground borne vibrations under the train moving loads and Byun *et al.* (2015) studied the conditions of railway substructure by a hybrid cone penetrometer. In other work, Wang *et al.* (2015) investigated the effects of embankment load on the settlement of railway foundation.

Reviewing the existing technical literature regarding to vehicle/track dynamic interaction models show that the stiffness effects in track substructure components have not been investigated in detail up to now. The pyramid model is an applicable substructure model considering the pyramid shape of stress distribution under the foundation which firstly was introduced by Ahlbeck *et al.* (1978). This model was successfully implemented in a vehicle/ track interaction model by Zhai *et al.* (2004). In their study, the substructure included only the ballast layer and did not consider the

∗Corresponding author, Associate Professor
E-mail: m_esmaeili@iust.ac.ir
[a]Ph.D.
E-mail: mosayebi@iust.ac.ir
[b]Professor
E-mail: zakeri@iust.ac.ir

ISSN: 1225-4568 (Print), 1598-6217 (Online)

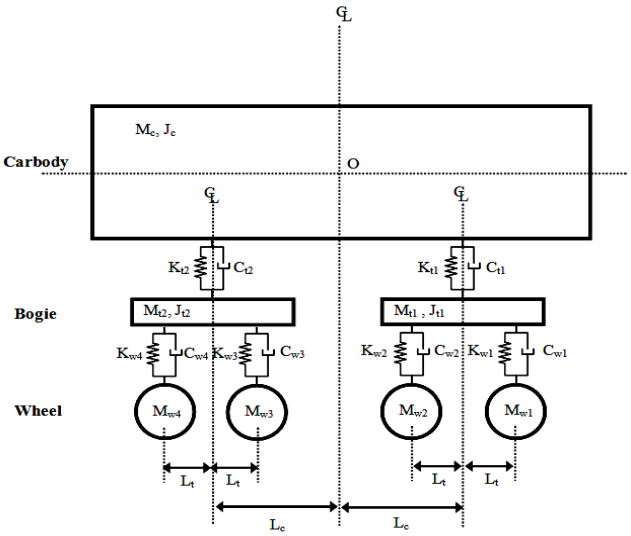

Fig. 1 Railway vehicle model

substructure components such as subgrade and embankment layers.

The present study is allocated to developing the previous studies of Zhai *et al.* (2004) model to obviate this shortage. Based on the different specifications of ballasted railway tracks such as ballast height, sleepers spacing and sleeper width, two different categories of track substructure stiffness model can be defined as types A and B. For ballasted track with rail, sleeper, ballast, subgrade and embankment layers, substructure stiffness model type A corresponds to the developed pyramid model of ballasted track by initiation the stress overlap areas in adjacent sleepers from the ballast layer while in type B the stress overlap areas originated from the subgrade layer. For this purpose, firstly the railway vehicle model including carbody, bogies and wheels is introduced. Then, the new substructure models for ballasted railway track with embankment layer including types A and B are presented and the stiffness equations related to A and B types are derived. In continuation, the railway track model with five layers including the embankment is simulated by using the finite element method. Then, this model under the moving train loads is analyzed. In the next stage, the type of new track substructure system is determined for various track specifications. Finally, a series of sensitivity analyses are performed on the track models with new substructure systems.

2. Vehicle-track interaction model

In this section, the numerical models of railway vehicle and track are presented. At first, the modeling of railway vehicle is described and then the new developed substructure models of ballasted railway are introduced.

2.1 Railway vehicle model

Firstly for modeling the railway vehicle, the motion equations of all vehicle parts are derived and then the mass,

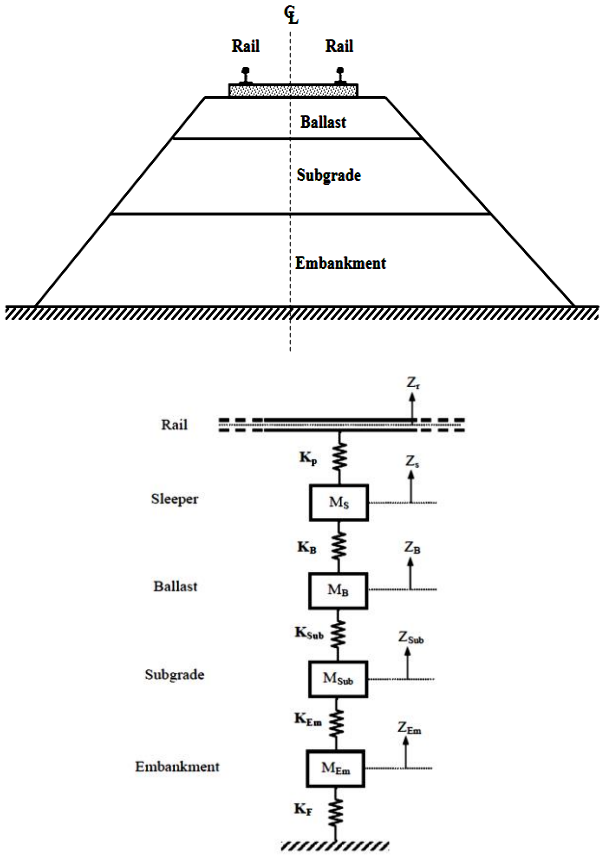

Fig. 2 Components of ballasted railway track

damping and the stiffness matrices of vehicle are extracted. Fig. 1 illustrates the railway vehicle configuration including carbody, bogies and wheels. This vehicle has 10 degrees of freedom including carbody with 2 degrees of freedom, each bogie with 2 degrees of freedom and each wheel with 1 degree of freedom (Zakeri and Xia, 2008), (Zakeri *et al.*, 2009).

In Fig. 1, parameters of "M", "J", "K" and "C" are mass, rotational moment of inertia, stiffness and damping of vehicle components respectively. Moreover, "L_t" and "L_c" are axis distance of bogie and wheel and axis distance of carbody and bogie respectively. Also in this paper, the specifications of vehicle are considered based on the Zakeri and Xia (2008) and Zakeri *et al.* (2009). In continuation, the details of new substructure models of ballasted railway are presented.

2.2 New substructure models for ballasted railway track with embankment

The main body of ballasted railway tracks contains several sections including rail, sleeper, ballast, subgrade and embankment. In the railway tracks, the ballast layer transfers the passing train loads to subgrade, works as drainage of surface waters, helps to leveling the rail surface, protects subgrade layer against freezing and restrains the vegetables growth in railway track. The role of subgrade layer is minimizing the amount of stress transferred from the ballast layer to embankment and reducing the imposed

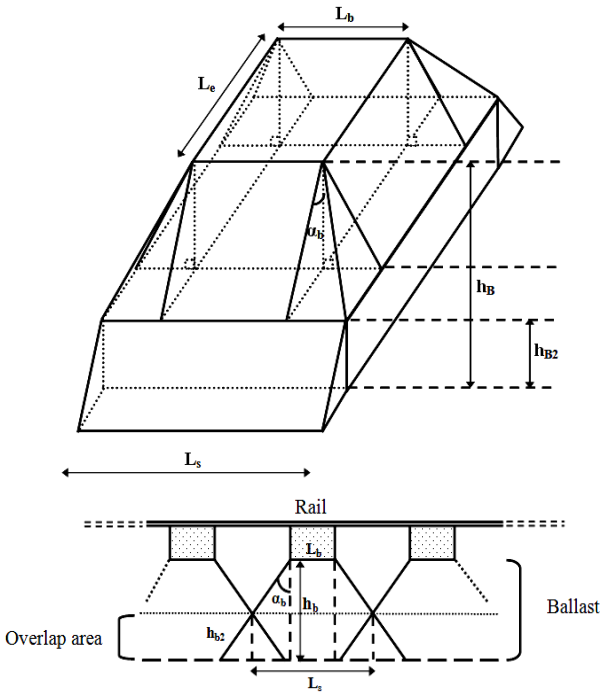

Fig. 3 Pyramid model in ballast layer

vibration from passing trains and resist against frost penetration. Also, the embankment body must be stable and satisfy the limitations of settlement during the passing of various trains (UIC Code 719R, 1994), (Leaflet No. 301, 2002). Fig. 2 shows a railway track with five components containing rail, sleeper, ballast, subgrade and embankment layers.

One of the applicable methods for calculating the stiffness of ballasted railway track layers is pyramid model. This method is based on the stress distribution under the sleeper (Zhai *et al.* 2004). Fig. 3 shows the pyramid model in the ballast layer considering the stress overlap area in this layer.

In Fig. 3, "h_b", "h_{b2}" and "α_b" are the total height, height of stress overlap area and the angle of stress distribution in the ballast layer respectively. Also, "L_s" is the sleepers spacing. According to pyramid model, the force transferred to sleeper is calculated as follows

$$Q = qL_eL_b \tag{1}$$

In this equation, "Q", "q", "L_e" and "L_b" are force, stress, the effective length and width of sleeper respectively. Then the layer strain and settlement are obtained as follows

$$\varepsilon_z = \frac{q_z}{E} \tag{2}$$

$$S = \int_0^h \varepsilon_z dz \tag{3}$$

In this equation, "ε_z", "q_z", "S" and "E" are strain, stress, settlement and the elastic modulus respectively. Therefore, the layer spring stiffness (K) is calculated by dividing the force to settlement as follows

Table 1 Mass and stiffness of ballast layer (Zhai *et al.* 2004)

Parameters	Equations
Mass	$M_B = \rho_B \begin{bmatrix} L_b h_B \left(L_e + h_B \tan\alpha_B\right) \\ +L_e \tan\alpha_B \left(h_B^2 - h_{B2}^2\right) \\ +\frac{4}{3}\left(h_B^3 - h_{B2}^3\right)\tan\alpha_B^2 \end{bmatrix}$
Stiffness (Without stress overlap area)	$K_{B1} = \frac{2\left(L_e - L_b\right)tg\,\alpha_B}{\ln\left[\left(\frac{L_e}{L_b}\right).\left(\frac{L_s}{L_e + 2h_{B1}\tan\alpha_B}\right)\right]}E_B$
Stiffness (With stress overlap area)	$K_{B2} = \frac{2L_s tg\,\alpha_B}{\ln\left[1 + \frac{2h_{B2}tg\,\alpha_B}{L_e + 2h_{B1}\tan\alpha_B}\right]}E_B$

$$K = \frac{Q}{S} \tag{4}$$

For track including the ballast layer, the ballast mass and stiffness are presented in Table 1.

According to the various specifications of ballasted railway tracks such as ballast height, sleepers spacing and sleeper width, there are two types A and B for track stiffness equations with new substructure systems. As shown in Fig. 4, in type A the stress distribution in depth starts beneath the adjacent sleepers but their stress overlaps start from ballast layer where as in type B the stress overlap area begins from subgrade layer. Fig. 4 shows the pyramid model configurations respect to type A substructure model. In Fig. 4, h_{B1}, h_{B2}, h_{Sub} and h_{Em} are the height of ballast layer without overlap area (first layer), ballast layer with stress overlap area (second layer), subgrade layer and embankment layer respectively. Also, K_{B1}, K_{B2}, K_{Sub} and K_{Em} are the stiffness of the mentioned track substructure layers. Fig. 5 presents the stress distribution pattern in pyramid model of type B substructure model.

In Fig. 5, h_B, h_{Sub1}, h_{Sub2} and h_{Em} are the height of ballast layer, subgrade layer without stress overlap area (first layer), subgrade layer with stress overlap area (second layer) and embankment layer respectively. Also, K_B, K_{Sub1}, K_{Sub2} and K_{Em} are the stiffness of the mentioned track substructure layers. Based on the developed pyramid models for railway track with new substructure system, their equations are derived. Tables 2 and 3 indicate the derived equations for two railway substructure models A and B respectively.

In these tables, the important parameters like "ρ", "h", "L_e", "L_b", "L_s", "α" and "E" are density, thickness, effective length of sleeper, width of sleeper, sleepers spacing, angle of stress distribution and elasticity modulus of railway track layers. For analysis the railway track under the moving train loads, a model of vehicle/railway track including new substructure system is developed. For this purpose, the railway track model with five layers is simulated by using the finite element method. In Fig. 6, this

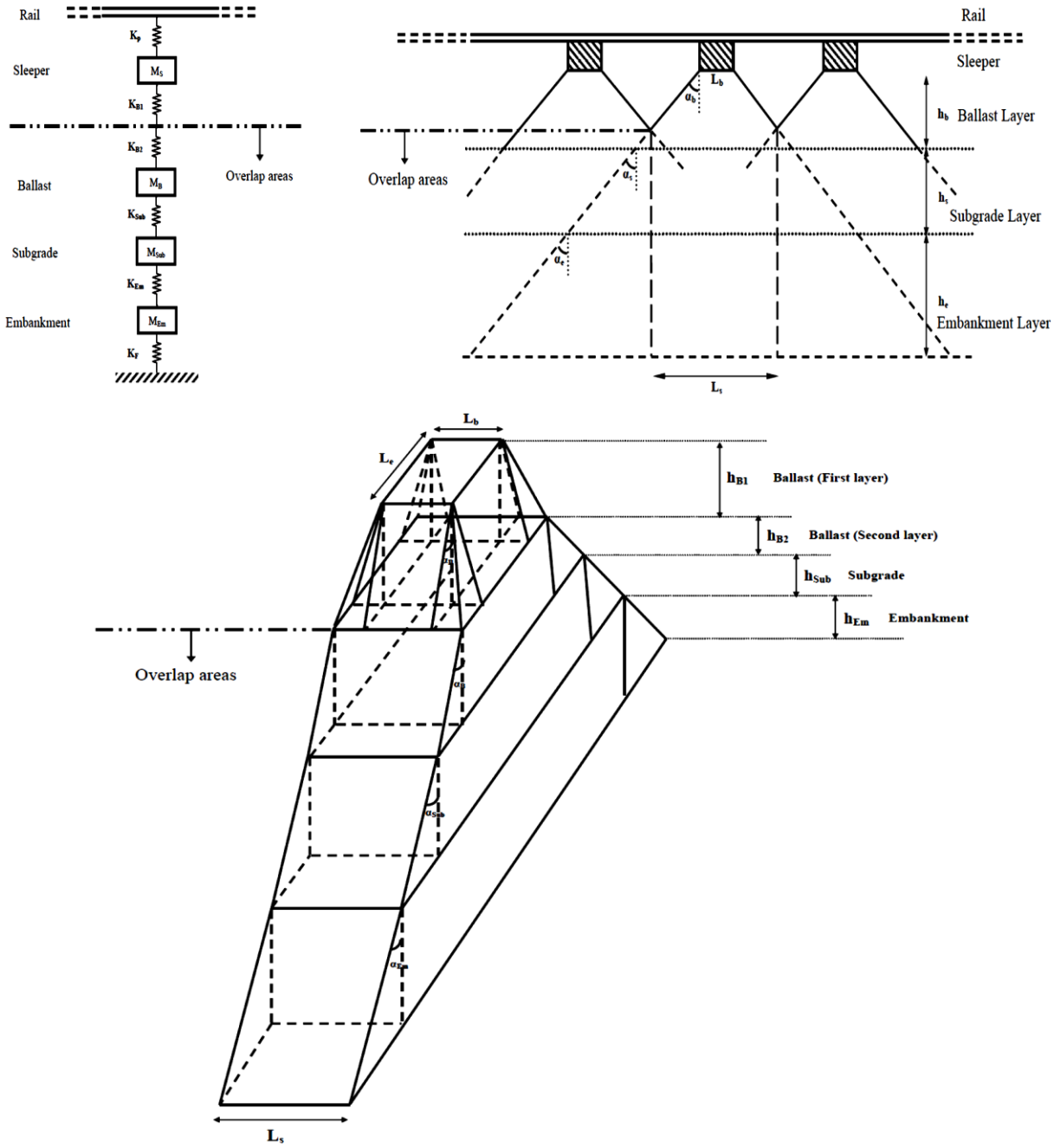

Fig. 4 Type A substructure model

track model including rail, sleeper, ballast, subgrade and embankment components is presented.

In this track model, K_p, K_B, K_{Sub}, K_{Em} and K_F are the stiffness of pad, ballast, subgrade, embankment and foundation respectively. Also, M_s, M_B, M_{Sub} and M_{Em} are the mass of sleeper, ballast, subgrade and embankment respectively.

3. Numerical model validation

For validating the present numerical model, a railway train-track dynamic interaction was modeled and the results were verified with the results of O'Brien *et al.* (2012). The obtained results from the present study and O'Brien *et al.* (2012) under moving train are presented in Fig. 7.

As shown in Fig. 7, the obtained results in present study have a good agreement with the results of O'Brien *et al.* (2012). In continuation, a series of sensitivity analyses are accomplished on the railway track with new substructure systems.

4. Sensitivity analysis on parameters of new substructure systems

In this section, a series of sensitivity analyses on parameters of new substructure systems are performed. In

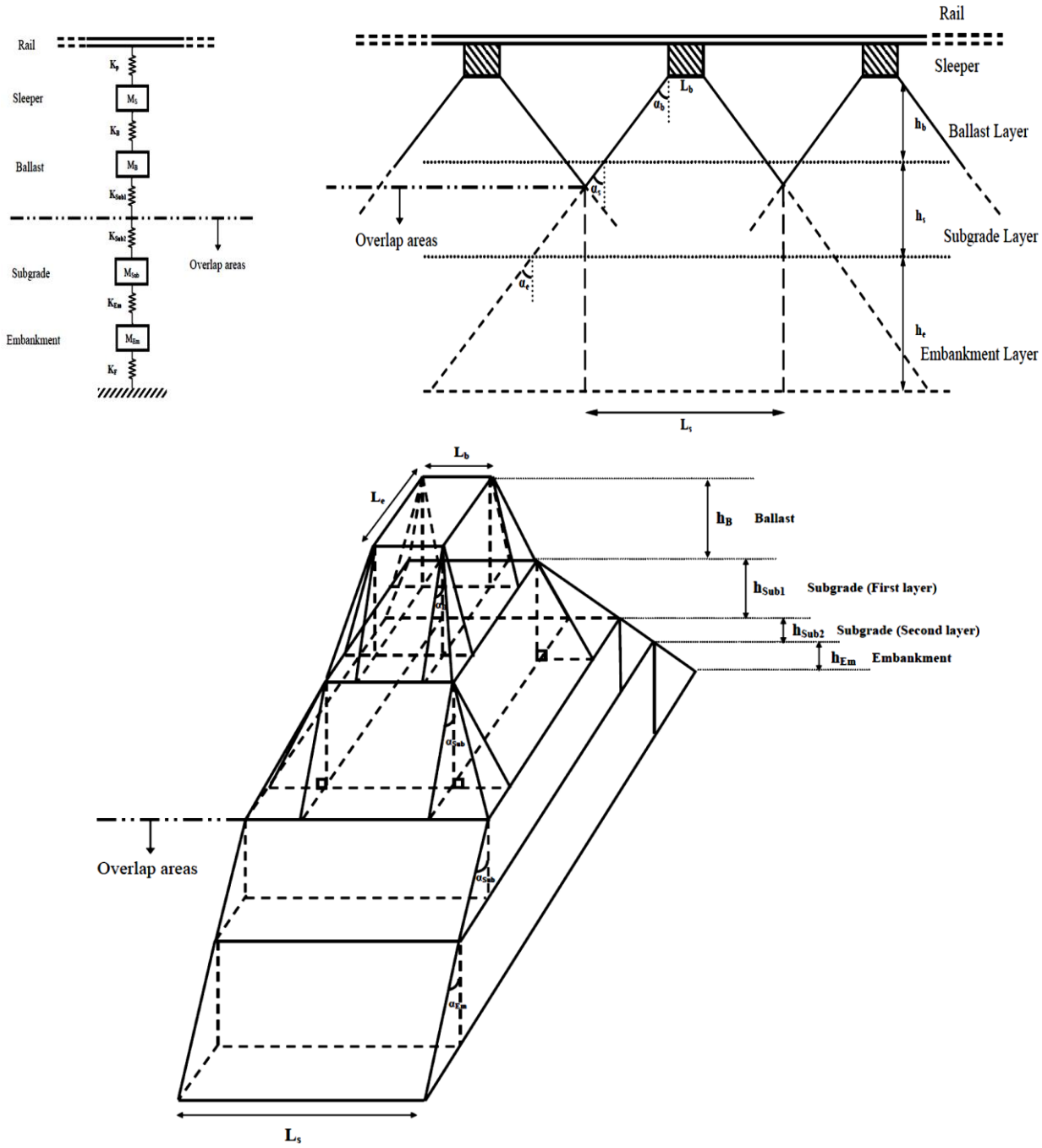

Fig. 5 Type B substructure model

this way, the type of railway substructure system should be determined for different track specifications. In this regard for evaluating the relevancy of types A or B substructure model, firstly the track parameters are substituted in equations derived for type A and consequently the overlap area in the ballast layer (h_{B2}) is calculated as follows

$$h_{B2} = h_B - \frac{L_s - L_b}{2\tan\alpha_B} \tag{5}$$

If this value (h_{B2}) is positive, the selected substructure model type A is correct otherwise the calculation is repeated for substructure model type B. This procedure for determining the type of new substructure system for each track specifications should be done until the type of substructure model to be specified. Table 4 indicates the dominant substructure model for various track specifications.

In continuation, two series of sensitivity analyses are presented corresponding to the effect of various track parameters on the track stiffness and the effect of track stiffness on vehicle/track dynamic interaction.

4.1 Effects of track parameters on track stiffness

Using the presented track parameters in Table 4, a series

Table 2 Derived equations for type A substructure model

Layers	Parameters	Equations
Ballast	Mass	$M_B = \rho_B \left[L_b h_B \left(L_e + h_B \tan\alpha_B \right) + L_e \tan\alpha_B \left(h_B^2 - h_{B2}^2 \right) + \frac{4}{3}\left(h_B^3 - h_{B2}^3 \right) \tan\alpha_B^2 \right]$
	Stiffness (Without stress overlap area)	$K_{B1} = \frac{2\left(L_e - L_b\right) tg\,\alpha_B}{\ln\left[\left(\frac{L_e}{L_b} \right) . \left(\frac{L_b + 2h_B tg\,\alpha_B}{L_e + 2h_B tg\,\alpha_B} \right) \right]} E_B$
	Stiffness (With stress overlap area)	$K_{B2} = \frac{2L_s tg\,\alpha_B}{\ln\left[1 + \frac{2h_{B2} tg\,\alpha_B}{L_e + 2h_{B1} \tan\alpha_B} \right]} E_B$
Subgrade	Mass	$M_{Sub} = \rho_{Sub} L_s h_{Sub} \left[L_e + 2h_{B1} \tan\alpha_B + 2h_{B2} \tan\alpha_B + h_{Sub} \tan\alpha_{Sub} \right]$
	Stiffness	$K_{Sub} = \frac{2L_s tg\,\alpha_{Sub}}{\ln\left[1 + \frac{2h_{Sub} tg\,\alpha_{Sub}}{L_e + 2h_{B1} \tan\alpha_B + 2h_{B2} \tan\alpha_B} \right]} E_{Sub}$
Embankment	Mass	$M_{Em} = \rho_{Em} L_s h_{Em} \left[L_e + 2h_{B1} \tan\alpha_B + 2h_{B2} \tan\alpha_B + 2h_{Sub} \tan\alpha_{Sub} + h_{Em} \tan\alpha_{Em} \right]$
	Stiffness	$K_{Em} = \frac{2L_s tg\,\alpha_{Em}}{\ln\left[1 + \frac{2h_{Em} tg\,\alpha_{Em}}{L_e + 2h_{B1} \tan\alpha_B + 2h_{B2} \tan\alpha_B + 2h_{Sub} \tan\alpha_{Sub}} \right]} E_{Em}$
Foundation	Stiffness	$K_F = L_s (L_e + 2h_{B1} \tan\alpha_B + 2h_{B2} \tan\alpha_B + 2h_{Sub} \tan\alpha_{Sub} + 2h_{Em} \tan\alpha_{Em}) E_F$

Table 3 Derived equations for type B substructure model

Layers	Parameters	Equations
Ballast	Mass	$M_B = \rho_B h_B \left[L_e L_b + L_e h_B \tan\alpha_B + L_b h_B \tan\alpha_B + \frac{4}{3} h_B^2 \tan\alpha_B^2 \right]$
	Stiffness	$K_B = \frac{2\left(L_e - L_b\right) tg\,\alpha_B}{\ln\left[\left(\frac{L_e}{L_b} \right) . \left(\frac{L_b + 2h_B tg\,\alpha_B}{L_e + 2h_B tg\,\alpha_B} \right) \right]} E_B$
Subgrade	Mass	$M_{Sub} = \rho_{Sub} \left[\begin{array}{l} (L_b + 2h_B \tan\alpha_B) h_{Sub} \left(L_e + 2h_B \tan\alpha_B + h_{Sub} \tan\alpha_{Sub} \right) \\ + (L_e + 2h_B \tan\alpha_B) \tan\alpha_{Sub} \left(h_{Sub}^2 - h_{Sub2}^2 \right) + \frac{4}{3}\left(h_{Sub}^3 - h_{Sub2}^3 \right) \tan\alpha_{Sub}^2 \end{array} \right]$
	Stiffness (Without stress overlap area)	$K_{Sub1} = \frac{2\left(L_e - L_b\right) tg\,\alpha_{Sub}}{\ln\left[\left(\frac{L_e + 2h_B \tan\alpha_B}{L_b + 2h_B \tan\alpha_B} \right) . \left(\frac{L_b + 2h_B \tan\alpha_B + 2h_{Sub1} tg\,\alpha_{Sub}}{L_e + 2h_B \tan\alpha_B + 2h_{Sub1} tg\,\alpha_{Sub}} \right) \right]} E_{Sub}$
	Stiffness (With stress overlap area)	$K_{Sub2} = \frac{2L_s tg\,\alpha_{Sub}}{\ln\left[1 + \frac{2h_{Sub2} tg\,\alpha_{Sub}}{L_e + 2h_B \tan\alpha_B + 2h_{Sub1} \tan\alpha_{Sub}} \right]} E_{Sub}$
Embankment	Mass	$M_{Em} = \rho_{Em} L_s h_{Em} \left[\begin{array}{l} L_e + 2h_B \tan\alpha_B + 2h_{Sub1} \tan\alpha_{Sub} \\ + 2h_{Sub2} \tan\alpha_{Sub} + h_{Em} \tan\alpha_{Em} \end{array} \right]$
	Stiffness	$K_{Em} = \frac{2L_s tg\,\alpha_{Em}}{\ln\left[1 + \frac{2h_{Em} tg\,\alpha_{Em}}{L_e + 2h_B \tan\alpha_B + 2h_{Sub1} \tan\alpha_{Sub} + 2h_{Sub2} \tan\alpha_{Sub}} \right]} E_{Em}$
Foundation	Stiffness	$K_F = L_s (L_e + 2h_B \tan\alpha_B + 2h_{Sub1} \tan\alpha_{Sub} + 2h_{Sub2} \tan\alpha_{Sub} + 2h_{Em} \tan\alpha_{Em}) E_F$

of sensitivity analyses are performed on the track substructure stiffness. Fig. 8 depicts the stiffness of ballast and embankment layers versus ballast height for sleepers spacing 60 cm.

Based on Fig. 8, the stiffness of ballast layer increases by increasing the sleeper width for all ballast height and it decreases by increasing the ballast height. Also, the embankment layer stiffness increases by increasing the

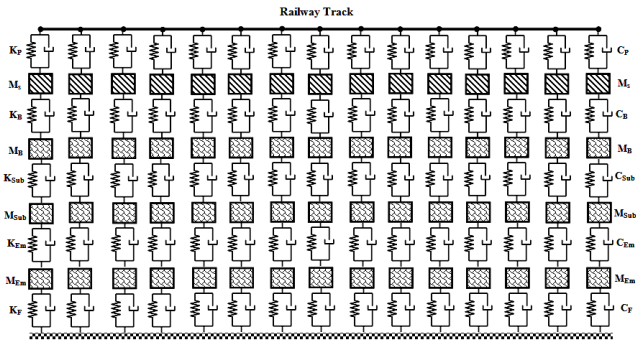

Fig. 6 Model of railway track with new substructure system

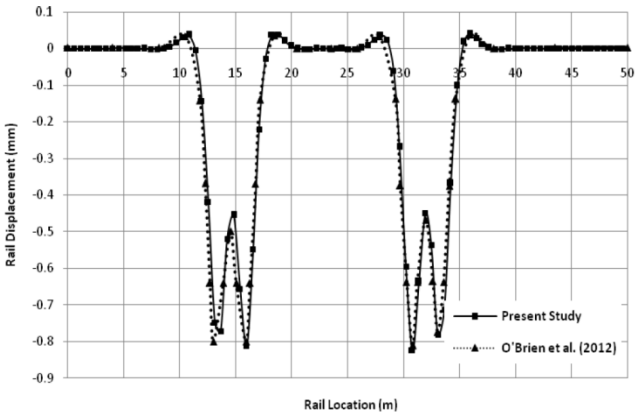

Fig. 7 The validation of numerical model

Table 4 The type of substructure model for various track specifications

Sleepers spacing (cm)	Ballast height (cm)	Sleeper width(cm)		
		20	25	30
50	20	B	A	A
	30	A	A	A
	40	A	A	A
	50	A	A	A
60	20	B	B	B
	30	A	A	A
	40	A	A	A
	50	A	A	A
70	20	B	B	B
	30	B	B	A
	40	A	A	A
	50	A	A	A
A	Type A substructure model			
B	Type B substructure model			

ballast height. Fig. 9 illustrates the stiffness of ballast and embankment layers versus sleepers spacing for ballast height 30 cm.

As can be observed from Fig. 9, the stiffness of ballast and embankment layers increases by increasing the sleepers spacing. Fig. 10 shows the stiffness of ballast and embankment layers versus ballast height for sleeper width 25 cm.

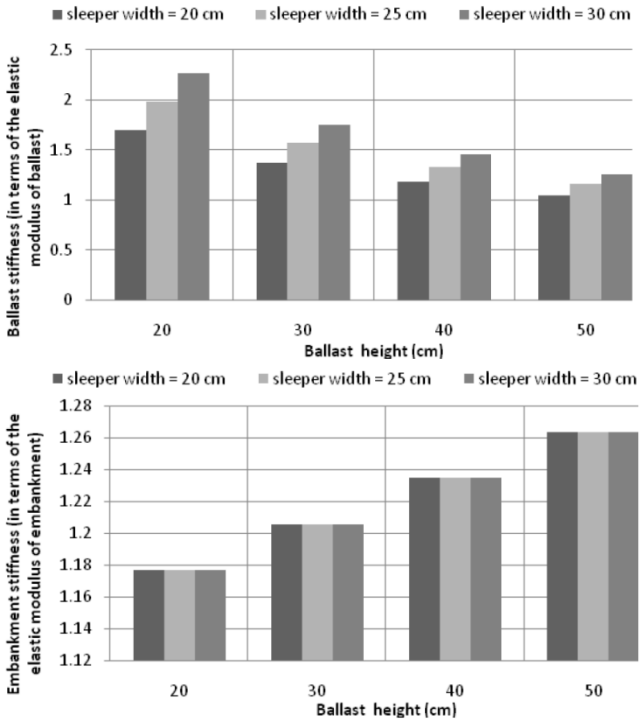

Fig. 8 Ballast and embankment layers stiffness for sleepers spacing 60 cm

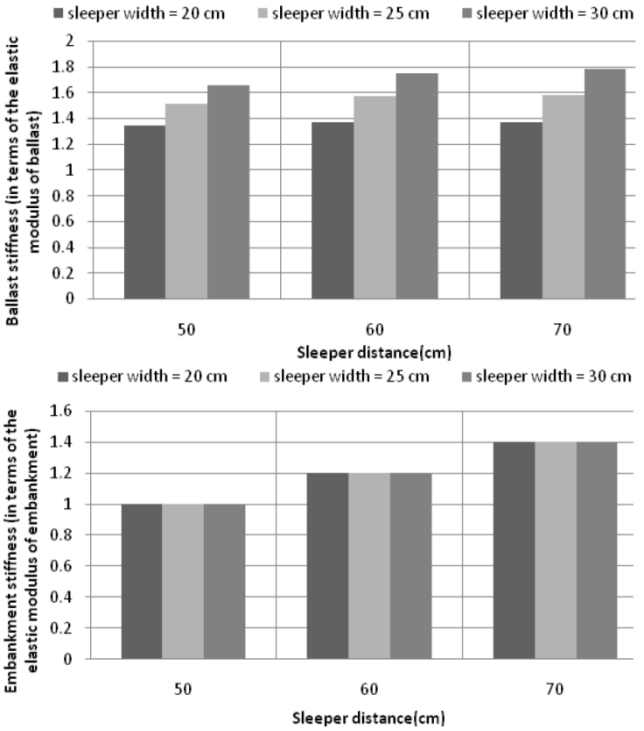

Fig. 9 Ballast and embankment layers stiffness for ballast height 30 cm

As can be seen from Fig. 10, the stiffness of ballast layer decreases by increasing the ballast height and it increases by increasing the sleepers spacing especially for the high ballast heights. Also, the embankment layer stiffness increases by increasing the ballast height and sleepers spacing.

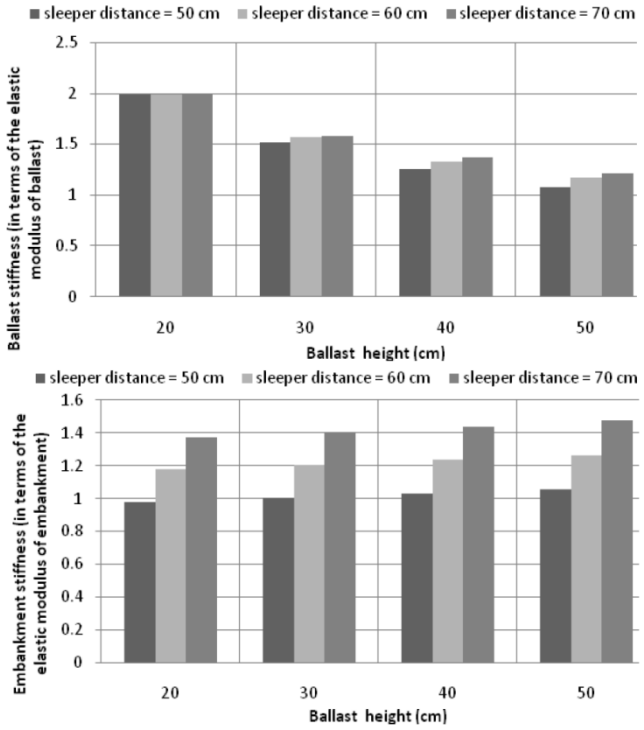

Fig. 10 Ballast and embankment layers stiffness for sleeper width 25 cm

Table 5 Ballasted track specifications (Zakeri and Xia 2008, Zakeri *et al.* 2009)

Parameter	Symbol	Value	Unit
Ballast Damping	C_B	120	kNs/m
Ballast elastic modulus	E_B	125	MPa
Pad Damping	C_P	140	kNs/m
Pad stiffness	K_P	140	MN/m
Subgrade damping	C_{Sub}	90	kNs/m
Subgrade elastic modulus	E_{Sub}	80	MPa
Embankment elastic modulus	E_{Em}	65	MPa
Embankment damping	C_{Em}	90	kNs/m
Foundation elastic modulus	E_F	45	MPa
Soil damping	C_F	40	kNs/m

4.2 Effects of track parameters on vehicle/track interaction

In this section, the results of sensitivity analyses on track specifications according to Table 4 are presented. Table 5 shows the dynamic specifications of components in ballasted track for analysis under moving train loads.

Fig. 11 indicates a sample of ballasted track response under the passing train. In this figure, the track specifications includes the ballast height of 20 cm, sleeper width of 20 cm and sleepers spacing of 60 cm which refers to type B substructure model according to Table 4.

As can be observed from Fig. 11, the vertical displacement of rail is more than other track components. Fig. 12 depicts the absolute maximum of rail and ballast

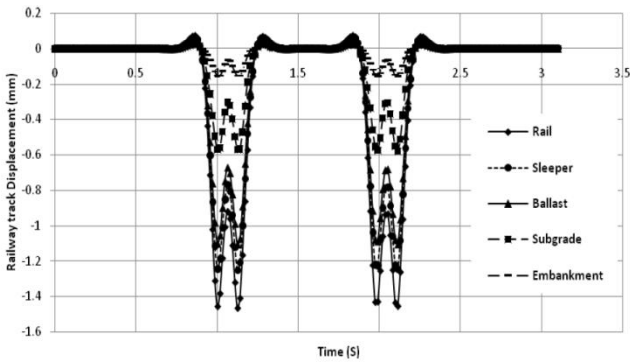

Fig. 11 Track response under the passing train

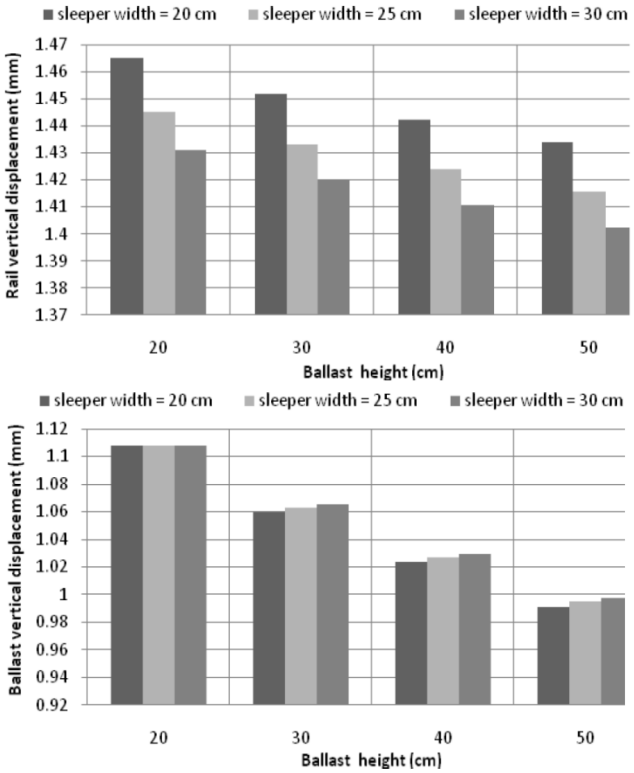

Fig. 12 Rail and ballast layers responses for sleepers spacing 60 cm

displacements versus ballast height for sleepers spacing 60 cm.

As can be seen from Fig. 12, the responses of rail and ballast layers decrease by increasing the ballast height. Also by increasing the sleeper width, the response values of rail decrease. Fig. 13 presents the responses of rail and embankment layers versus sleepers spacing for ballast height of 30 cm.

Based on Fig. 13, rail vertical displacements increase by increasing the sleepers spacing. Also, the response of embankment decreases with the increase in sleepers spacing. Fig. 14 presents the responses of rail and embankment layers versus ballast height for sleeper width of 25 cm.

According to Fig. 14, the displacement of rail decreases by increasing the ballast height. Also, the responses of embankment layer decrease with increase of ballast height.

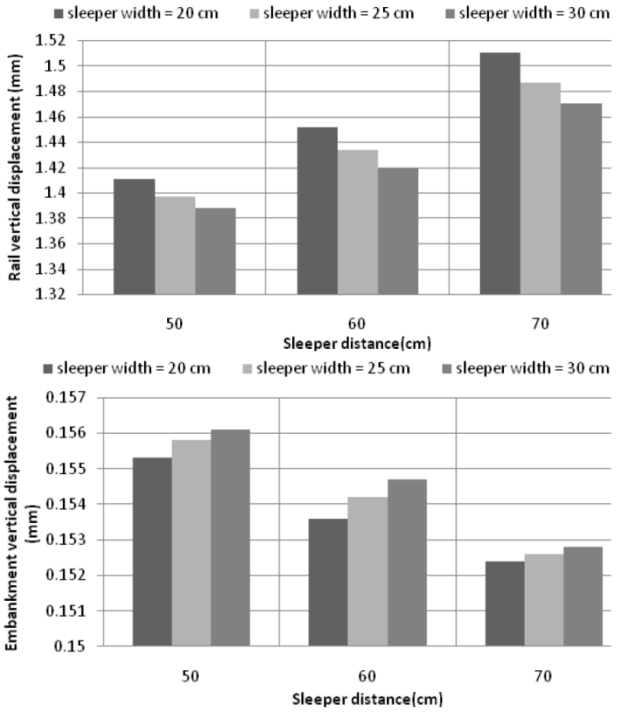

Fig. 13 Rail and embankment layers responses for ballast height 30 cm

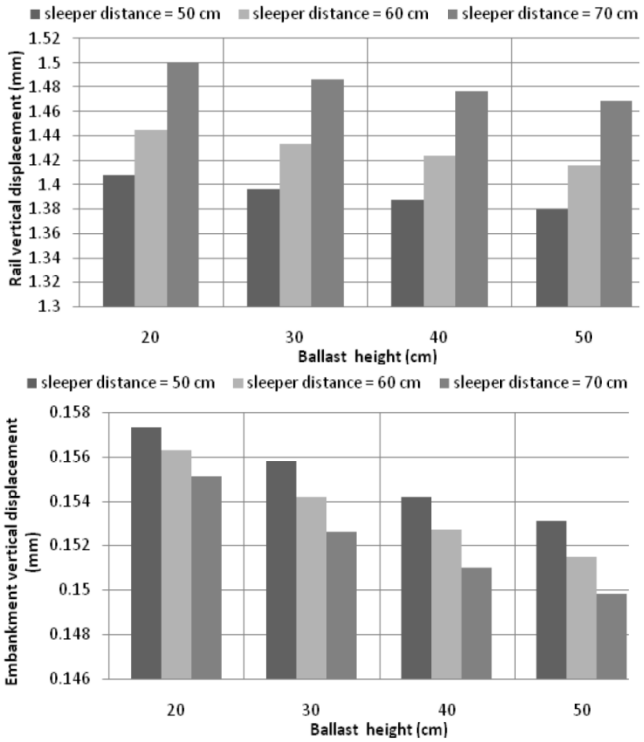

Fig. 14 Rail and embankment layers responses for sleeper width 25 cm

5. Conclusions

In this paper, firstly the models of railway vehicle and ballasted track were presented. The model of railway vehicle included carbody, bogies and wheels. Then, many new substructure models of ballasted railway track were developed. Based on various ballasted track specifications, two different categories of new substructure models were introduced. The substructure model type A covers the ballasted track with multi components including embankment layer by initiation of the stress overlap area in adjacent sleepers from the ballast layer while in substructure model type B, the stress overlap areas take placed in subgrade layer. According to substructure models type A or B, the relevant equations of pyramid model were derived. In the next stage, the model of ballasted track including multi components under the moving train loads was simulated and solved and verified by using the finite element method. In continuation, a series of sensitivity analyses on parameters of new substructure models and the railway track system were accomplished and consequently the following important finding were achieved:

- Two types of track substructure models were presented for various track specifications. For example, the track substructure type was B for sleepers spacing of 50 cm, ballast height of 20 cm and sleeper width of 20 cm while the railway substructure type was A if sleeper width was 30 cm.
- The ballast stiffness decreased by increasing the ballast height. For sleepers spacing 60 cm, the stiffness of ballast layer decreased 38.2, 41.3 and 44.3 percent by increasing the ballast height from 20 to 50 cm for sleeper widths 20, 25 and 30 cm respectively.
- The stiffness of subgrade, embankment and foundation increased by increasing the ballast height. By increasing the ballast height from 20 to 50 cm, the stiffness of subgrade, embankment and foundation increased by 20, 7.42 and 5.1 percent respectively.
- The stiffness of ballast layer increased by increasing the sleeper width. For sleepers spacing 60 cm, the ballast stiffness increased by 33.4, 28.1, 23.3 and 20.2 percent by increasing the sleeper width from 20 to 30 cm for ballast heights of 20, 30, 40 and 50 cm respectively. Also, The mass of ballast layer increased by increasing the sleeper width. For sleepers spacing 60 cm, the ballast mass increased by 29, 20.1, 13.4 and 9.5 percent by increasing the sleeper width from 20 to 30 cm for ballast height 20, 30, 40 and 50 cm respectively.
- The ballast layer stiffness increased by increasing the sleepers spacing. For sleeper width 25 cm, the ballast stiffness increased 0.2, 4.1, 8.9 and 12.3 percent by increasing the sleepers spacing from 50 to 70 cm for ballast height 20, 30, 40 and 50 cm respectively.
- The stiffness of embankment layer increased by increasing the sleepers spacing. By increasing the sleepers spacing from 50 to 70 cm, the embankment stiffness increased by 40 percent.
- By increasing the ballast height, rail and ballast vertical displacement decreased. The responses of rail and ballast decreased 2 and 10 percent with increase of ballast height from 20 to 50 cm respectively.
- The response of rail increased by increasing the sleepers spacing. By increasing the sleepers spacing from 50 to 70 cm, the rail vertical displacement increased 6.5 percent.

References

Ahlbeck, D.R., Meacham, H.C. and Prause, R.H. (1978), "The development of analytical models for railroad track dynamics", Ed. Kerr, A.D., *Railroad Track Mechanics & Technology*, Pergamon Press, Oxford.

Berggren, E.G. (2009), "Railway track stiffness-dynamic measurements and evaluation for efficient maintenance", PhD Thesis, Royal Institute of Technology, Sweden.

Byun, Y.H., Hong, W.T. and Lee, J S. (2015), "Characterization of railway substructure using a hybrid cone penetrometer", *Smart Struct. Syst.*, **15**(4), 1085-1101.

Cai, Z. and Raymond, G.P. (1994), "Modelling the dynamic response of railway track to wheel/rail impact loading", *Struct. Eng. Mech.*, **2**(1), 95-112.

Chang, T.P. and Liu, Y.N. (1996), "Dynamic finite element analysis of a nonlinear beam subjected to a moving load", *Int. J. Solid. Struct.*, **33**(12), 1673-1688.

Esmaeili, M., Zakeri, J.A. and Mosayebi, S.A. (2014), "Effect of sand-fouled ballast on train-induced vibration", *Int. J. Pave. Eng.*, **15**(7), 635-644.

Ishida, M. and Suzuki, T. (2005), "Effect on track settlement of interaction excited by leading and trailing axles", *QR RTRI*, **46**(1), 1-6.

Kerr, A.D. (2000), "On the determination of the rail support modulus k", *Int. J. Solid. Struct.*, **37**(32), 4335-4351.

Kerr, A.D. (2003), *Fundamentals of Railway Track Engineering*, Simmons-Boardman Books, Incorporated.

Leaflet No. 301, (2002), *Technical and General Specification of Ballasted Railway*, Management and Planning Organization of Iran, Tehran, Iran.

Lei, X. and Zhang, B. (2010), "Influence of track stiffness on vehicle and track interactions in track transition", *Proceedings of the Institution of Mechanical Engineers, Part F: Journal of Rail and Rapid Transit*, **224**(6), 592-604.

Muscolino, G. and Palmeri, A. (2007), "Response of beams resting on viscoelastically damped foundation to moving oscillators", *Int. J. Solid. Struct.*, **44**(5), 1317-1336.

O'Brien, E.J., Taheri, A. and Gavin, K. (2012), "The influence of subgrade subsidence on train track dynamic interaction", in J. Pombo, (Editor), *Proceedings of the First International Conference on Railway Technology*: Research, Development and Maintenance, *Civil-Comp Press*, Stirlingshire, UK, Paper 110, doi:10.4203/ccp.98.110.

Rezvani, M.A., Vesali, F. and Eghbali, A. (2013), "Dynamic response of railway bridges traversed simultaneously by opposing moving trains", *Struct. Eng. Mech.*, **46**(5), 713-734.

Sun, Y.Q. and Dhanasekar, M. (2002), "A dynamic model for the vertical interaction of the rail track and wagon system", *Int. J. Solid. Struct.*, **39**(5), 1337-1359.

UIC Code 719R, International Union of Railways, (1994), *Earthworks and Track-bed Layers for Railway Lines*, 2nd Edition, Paris, France.

Uzzal, R.U.A., Ahmed, W. and Rakheja, S. (2008), "Dynamic analysis of railway vehicle-track interactions due to wheel flat with a pitch-plane vehicle model", *J. Mech. Eng.*, **39**(2), 86-94.

Wang, C., Zhou, S., Wang, B., Guo, P. and Su, H. (2015), "Differential settlements in foundations under embankment load: Theoretical model and experimental verification", *Geomech. Eng.*, **8**(2), 283-303.

Xia, H., Deng, Y., Xia, C., De Roeck, G., Qi, L. and Sun, L. (2013), "Dynamic analysis of coupled train-ladder track-elevated bridge system", *Struct. Eng. Mech.*, **47**(5), 661-678.

Zakeri, J.A. and Ghorbani, V. (2011), "Investigation on dynamic behavior of railway track in transition zone", *J. Mech. Sci. Technol.*, **25**(2), 287-292.

Zakeri, J.A. and Xia, H. (2008), "Sensitivity analysis of track parameters on train-track dynamic interaction", *J. Mech. Sci. Tech.*, **22**(7), 1299-1304.

Zakeri, J.A., Xia, H. and Fan, J.J. (2009), "Dynamic responses of train-track system to single rail irregularity", *Latin Am. J. Solid. Struct.*, **6**(2), 89-104.

Zhai, W.M., Wang, K.Y. and Lin, J.H. (2004), "Modelling and experiment of railway ballast vibrations", *J. Sound Vib.*, **270**(4-5), 673-683.

PL